



ELSEVIER

Journal of Chromatography B, 697 (1997) 195–205

JOURNAL OF  
CHROMATOGRAPHY B

Review

## Non-isocratic capillary electrophoresis for detection of DNA point mutations

Pier Giorgio Righetti<sup>a,\*</sup>, Cecilia Gelfi<sup>b</sup>

<sup>a</sup>University of Verona, Department of Agricultural and Industrial Biotechnologies, Strada Le Grazie, Cà Vignal, 37134 Verona, Italy

<sup>b</sup>ITBA, CNR, Via Ampère 56, Milan, Italy

### Abstract

Capillary electrophoresis under non-isocratic conditions is reviewed here. In particular, these conditions are elicited by programming the temperature over the run, just as in temperature-programmed gas chromatography. There is at least one major instance in which this technique is particularly useful: detection of DNA point mutations in PCR-amplified DNA fragments. In this case, migration of DNA homo- and hetero-duplexes against a denaturing gradient (either thermal or chemical) is the only technique capable of developing a pattern of four zones, indicative of the presence of a point mutation in genomic DNA, and due to the formation of two homo- ( $W_1/W_1$ ,  $M/M$ , where  $W_1$ =wild type and  $M$ =mutant) and two hetero- ( $W_1/M$  and  $W_1/M$ ) duplexes, formed by fully denaturing and then re-annealing the  $W_1$  and  $M$  filaments in solution. It is demonstrated that it is possible to obtain such gradients (which do not exist in space, i.e., along the length of the capillary, but in time), simply by producing voltage ramps, which in turn generate temperature ramps from within the capillary lumen, rather than from without, by circulating liquids and thermostats. This technique can be applied to any possible type of mutation, from low- to intermediate to high-melters, i.e., from 40°C up to 60–65°C. Examples of separations of point mutations in the cystic fibrosis transmembrane regulator gene and in the  $\beta$ -globin chain gene are shown. ©1997 Elsevier Science B.V.

**Keywords:** Reviews; Point mutations; DNA

### Contents

1. Introduction .....	196
2. On the use of sieving liquid polymers .....	196
3. On the DGGE technique .....	198
4. Temperature-programmed capillary electrophoresis .....	199
5. Examples of separations of low- to high-melters by non-isocratic CZE .....	200
6. A glimpse at the future .....	204
7. List of abbreviations and symbols .....	204
Acknowledgments .....	204
References .....	204

\*Corresponding author. Address for correspondence: L.I.T.A., Via Fratelli Cervi 93, Segrate 20090, Milan, Italy.

## 1. Introduction

Small alterations in DNA sequence of genomic material lead to many human diseases, such as cancer, diabetes, heart disease, myocardial infarction, atopy, atherosclerosis, cystic fibrosis, Alzheimer, Duchenne muscular dystrophy, thalassemias. These alterations in DNA sequence include many types of mutations and polymorphisms in genomic material, such as substitutions of one or several nucleotides, deletions or insertion of some sequence, differences in variable number of tandem repeats (VNTR) and the genomic instability of microsatellite repeat [1]. DNA diagnosis for human diseases has thus very important applications in the fields of genetic and medical research, clinical chemistry and forensic science. Since a large portion of sequence variations in the human genome are caused by single base changes, any method used to detect mutations or polymorphisms must be capable of detecting single-base substitutions.

Up to recent times, slab gel electrophoresis has been the standard method for analysis of PCR products in the screening of genetic diseases, but the technique is time consuming, labor-intensive and unwieldy for precise quantitation. Particularly vexing is the fact that, at the end of the electrophoretic step, many manipulations are still involved for producing the final diagnostic data, such as gel slab staining (and destaining in silvering techniques), photographing and densitometry. This is why capillary zone electrophoresis (CZE) is rapidly emerging as a unique tool for analysis of gene defects [2]. CZE represents a fully automated version of electrophoresis, with such valuable features as on-line detection and quantitation of analytes, minute sample requirements, automatic sample injection, large analyte handling capability in the case of capillary arrays [3–5] and drastically reduced analysis times in the case of microfabricated chips [6,7] and/or when adopting isoelectric buffers [8]. Just to have an idea of the growing importance of CZE, one can note that, in a recent issue of *Electrophoresis*, entirely dedicated to nucleic acid electrophoresis [9], out of 15 papers, only four deal with gel electrophoresis, the other eleven being fully devoted to CZE analysis. A large body of data already exists on the analysis of genetic defects by CZE. Fortunately, two in-depth

reviews have appeared covering these aspects, to which the readers are referred [10,11]. The present review will be limited to some unique methodology our group has recently developed, namely the possibility of using CZE under non-isocratic conditions, precisely for temperature programmed runs (much like in the related version proposed 30 years ago in gas chromatography) for spotting point mutations in genomic DNA. The review will end with another, more advanced non-isocratic technique (at the moment only available in the gel slab format) i.e., the use of double gradients (chemical and porosity or thermal and porosity) or even triple gradients (chemical, thermal and of porosity) for detecting point mutations of such minute physico-chemical differences in melting point ( $T_m$ ) which often go undetected. Prior to expounding on this topic, we will briefly deal with two important aspects of the technique: the properties of sieving liquid polymers, as today routinely adopted in CZE for all DNA separations, and the basic concepts underlying denaturing gradient gel electrophoresis (DGGE), which is at the heart of our non-isocratic methodology.

## 2. On the use of sieving liquid polymers

Due to the fact that the standard cross-linked polyacrylamide gel, when prepared in a capillary lumen, often produced disastrous results (mostly due to micro air bubbles trapped in the matrix caused by the heat of polymerization and to matrix contraction), modern technologies are based solely on the use of liquid polymers, prepared in the absence of any cross-linker. A host of these polymer networks have been described, mainly for separation of double-stranded (ds) DNA. Such materials include methyl cellulose (MC) [12–14], hydroxyethyl cellulose (HEC) [15–18], hydroxypropyl cellulose [13], hydroxypropylmethyl cellulose (HPMC) [13], poly(ethylene glycol) (PEG) [19], poly(ethylene oxide) (PEO) [20], poly(vinyl alcohol) [16], liquid [21] or liquid/solid [22] agarose and glucomannan [23]. Typically, these polymers are used at concentrations in the 0.1–1.0% range, the lower levels (0.1–0.2%) being preferred for large DNA fragments (e.g., 5000 to 50 000 bp) the higher amounts (0.7–1.0%) being adopted for resolving shorter DNAs (e.g., 100 to 500

bp). However, by far, for the best separation of short DNA fragments and for DNA sequencing, the matrix of choice appears to be polyacrylamide, first proposed, at low and zero% cross-link, in 1990 by Heiger et al. [24]. Liquid linear polyacrylamide, however, suffers from many drawbacks: first of all, at the typical concentrations for proper DNA sieving (6–10%) it is extremely viscous and unwieldy to pumping processes; secondly, at the pH values of DNA electrophoresis (pH 8.2) and at the high temperatures utilized by us for detection of point mutants, it rapidly hydrolyses, producing polyacrylate. The latter, being charged, starts migrating out of the capillary lumen and it adds to the background buffer conductivity. “Hot spots” develop along the capillary length, producing air bubbles and cutting the electric current. Migration reproducibility, moreover, cannot be guaranteed any longer. Our group has proposed, over the years, several remedies: viscosity can be dramatically decreased by producing “fluidified” or “short-chain” ( $M_w$  of ca. 250 000,  $M_n$  of ca. 55 000, polydispersity=4.2) polyacrylamides, by polymerizing the monomer in presence of a chain-transfer agent (e.g., 3% 2-propanol) and at high temperatures (70°C) [25]. Hydrolysis-resistant monomers can cure the proneness to degradation typical of plain acrylamide. *N*-substituted acrylamides appear most suited from this point of view. Originally, we proposed *N*-acryloylaminoethoxy ethanol (AAEE), combining an extreme resistance to hydrolysis (by almost three orders of magnitude!) with an even greater hydrophilicity [26]. However, after finding that this monomer had the noxious habit of auto-polymerizing and auto-reticulating, we synthesized a series of  $\Omega$ -hydroxy, *N*-substituted acrylamides, notably *N*-acryloylamino propanol (AAP) and *N*-acryloylamino butanol (AAB) [27–29]. Additionally, we proved that the performance in DNA separations was even ameliorated in mixtures of these monomers, such as 5% AAP spiked with 1% AAB [30]. Moreover, in a recent report [31], we have compared the performance of our novel poly(acrylamides) with that of celluloses, at both room temperature and at 60°C. Contrary to previously held belief, which attributed best separations in poly(acrylamides) to small DNA fragments (typically in the 50 to 1000 bp size range) and in celluloses to large DNA fragments, it was

shown that celluloses can also achieve fine sieving of short DNA sizes provided they are used at much higher concentrations than previously reported. E.g., in the case of HEC, typically used at 0.2 to 0.8% concentrations, levels of 3% produce excellent patterns, at 25°C, in the 50 to 600 bp size range. If separations are conducted at 60°C, sieving is lost in most liquid polymers. However, if the concentration of HEC is raised to 6%, and that of HPMC above 1%, sieving is fully restored. Also our *N*-substituted acrylamido derivatives, notably AAEE and AAP, offer excellent performance at both 25 and 60°C, whereas plain poly(acrylamide) irreversibly collapses at high temperatures, possibly due to intrinsic instability of the amido bond under such harsh conditions. Among all the polymers investigated, an 8% solution of poly(AAP) was found to offer the best performance and the highest theoretical plate numbers in the 25 to 60°C interval. Such separations at high temperatures are necessary when dealing with detection of point mutations in temperature-programmed CZE (as shown in the present report) and are preferred in DNA sequencing [32]. Most recently, other types of polymers have been proposed for DNA analysis. In one report, telechelic polymers have been suggested [33]. They are formed by a central, linear water soluble polymer bearing hydrophobic end groups, as employed in the paint industry as rheology modifiers. A typical material consists of poly(ethylene glycol)s (e.g., PEG 35 000), end-capped with micelle-forming fluorocarbon tails, such as  $C_6F_{13}$  and  $C_8F_{17}$ . Above the critical micellar concentration, such telechelic polymers associate into purely intramolecular, rosette-like micellar structures. As the polymer concentration is increased, the rosettes transform into micellar aggregates through intermolecular micellization. As aggregates become larger and more concentrated, a continuous network ensues, held together by the hydrophobic micelles, that is able to efficiently sieve even small DNA chains as generated in sequencing reactions. The advantage of this polymeric material: under a high shear rate, as produced when filling a capillary lumen, there is a pronounced shear thinning (i.e., the network, which per se is highly viscous, is disrupted) thus rendering this otherwise viscous solution highly flowable. At rest, i.e., once the capillary is filled, the very short relaxation time of this polymer solution

(66 ms) allows a rapid regeneration of the network. In another approach, Sassi et al. [34] have proposed thermo-reversible matrices. These matrices combine the ease-of-use of agarose with the resolving properties of polyacrylamides. Two classes of matrices have been produced: (a) aqueous suspensions of gel microspheres; (b) solutions containing uncross-linked temperature-sensitive polymers (such as prepared with *N*-substituted, hydrophobic acrylamides of the type *N*-isopropyl acrylamide or *N,N'*-diethyl acrylamide). When heated, the viscosity of these solutions drops dramatically because of the phase-transition behaviour of these polymers, and therefore these formulations are easy to pour or load. Finally, in order to improve the sieving properties of such liquid matrices, mixed entangled polymer systems have been proposed [35]. As shown by Isenberg et al. [35], in order to improve separation of the products of a multiplex amplification of the loci DIS80 and amelogenin, a strategy of "titrating" a constant concentration of high  $M_n$  HEC (140 000) with increasing amounts of low  $M_n$  HEC (40 000) can be adopted. Optimum resolution in their DNA size interval was obtained in a mixture of 0.28% high  $M_n$  HEC and 0.3% low  $M_n$  HEC. In the case of conventional or *N*-substituted poly(acrylamides), however, this strategy did not improve the pattern at all. This is probably due to the fact that liquid poly(acrylamides) are already a mixture of low- and high-molecular-mass chains (in all cases the polydispersity, i.e., the ratio  $M_w/M_n$  is  $>4$ ; but this applies even more to HEC, where some batches display a polydispersity  $>10!$ ).

### 3. On the DGGE technique

Among the different methods available for revealing DNA point mutants, denaturing gradient gel electrophoresis (DGGE), as originally described by Myers et al. [36], has become one of the most popular techniques. DGGE involves the electrophoresis of double stranded (ds) DNAs in a polyacrylamide gel containing increasing concentrations of denaturing agents such as formamide, urea or temperature [37], and exploits the melting properties of the DNA molecule as a separation mechanism. DNA melts in domains at a temperature ( $T_m$ ) which

is dependent on the nucleotide sequence of the fragment under study. At the point along the gradient where the DNA fragment undergoes partial denaturation, its electrophoretic mobility will be strongly retarded (as a consequence of the entanglement of branched DNA molecules with the polyacrylamide matrix), thus allowing separation of two ds molecules differing by a single nucleotide in the domain with the lowest  $T_m$ . This is due to the fact that, rather than melting in a continuous zipper-like manner, most fragments melt in a step-wise process within a very narrow range of denaturing conditions. However, DNA segments differing by base changes within the domain with the highest  $T_m$  cannot be resolved in this way, since reaching the highest  $T_m$  would bring about complete strand dissociation. This can be overcome by introducing, during PCR, a G–C-rich domain (G–C-clamp) at the 5' end of one of the two ampli-primers. The DNA from an individual heterozygous for a mutation or polymorphism will show four bands on DGGE. The two faster migrating bands are the homoduplexes, corresponding to the wild type ( $W_1/W_1$ ) and the mutant ( $M/M$ ) alleles. The two additional bands that migrate at a slower rate in the gel consist of the two heteroduplexes formed by re-assorting of strands during PCR. Fig. 1 explains the basic principles of DGGE. It is seen that the two homo- and heteroduplexes are formed by amplifying separately the wild-type and the mutant DNA, fully denaturing the ds- to ss-DNAs and mixing them. Upon cooling, the spectrum of four bands forms. As they are electrophoresed down the length of a gel containing a denaturing gradient, they melt differentially, so as to be resolved into the typical four-zone pattern. It should be noted that the two heteroduplexes, due to the mismatch reverberating along a more extended domain in the double helix, are the first ones to melt [38]. The melting behaviour can be predicted by using the computer algorithm developed by Lerman and Silverstein [39]. Fig. 2 gives an example of the melting profile of a point mutation in thalassemia, in exon IIIB. The lower melting region has a very flat profile (which is very advantageous from an analytical point of view, since it means a very sharp melting point and thus the generation of a narrow electrophoretic zone) with a  $T_m$  value of 73.3°C. The high melting region (i.e., the stretch of the first 44

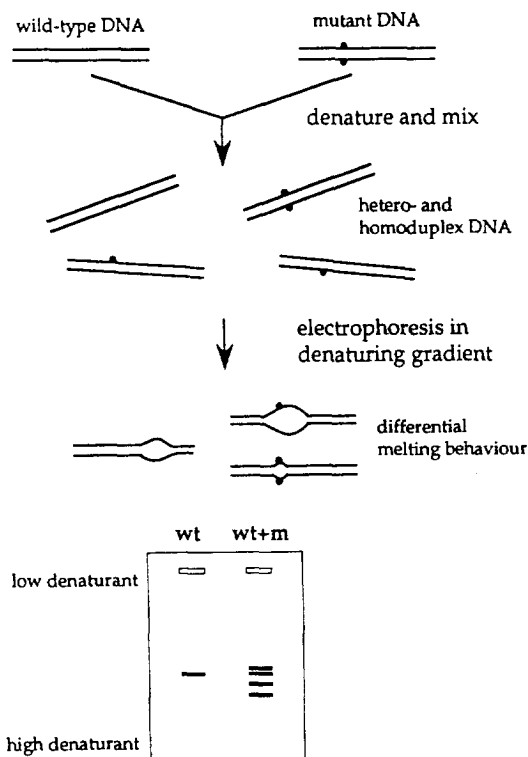


Fig. 1. The principle of DGGE. Wild-type ( $W_1$ ) and mutant ( $M$ ) PCR products are denatured and reannealed to generate four species: two homo- and two hetero-duplexes. Differential melting behaviour (as shown by the extent of the emias) leads to altered migration in a gradient of denaturing agents and to resolution of the envelope of four zones. Conversely, the wild-type homoduplex seeded in the left pocket originates only a single band. Total dissociation into single filaments as the zones progressively migrate into gel regions of higher denaturants is prevented by the G–C clamps at one extremity (Grompe, see Ref. [38], with permission).

bases) is the G–C clamp extremity which impedes total fusion into single stranded filaments (which would mean total loss of resolution).

#### 4. Temperature-programmed capillary electrophoresis

How is a temperature gradient generated inside a capillary and how is it optimized for detection of DNA point mutations? In gel-slab DGGE, as described by Riesner et al. [37], the temperature gradient exists in the separation space, i.e., the gel

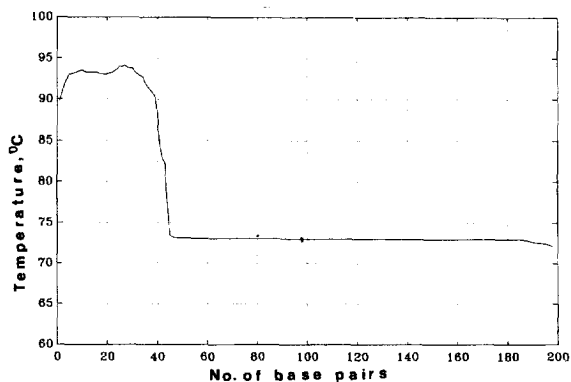


Fig. 2. Melting profile, as calculated with the Lerman and Silverstein program [39], of fragment IIIB (200 bp) carrying a C→T mutation in codon 39 of the  $\beta$ -globin gene. Note the sharp  $T_m$  value of 73.3 and the very flat profile of the low-melting region. The high melting region to the left represents the G–C clamp domain (Gelfi and Righetti, unpublished).

slab is placed on a heat-dissipating block under the action of two thermostats: one set at a lower (e.g., 55°C) and one set at a higher (e.g., 70°C) temperature. These two temperatures are applied at the cathodic and anodic gel extremities, respectively, and then a linear  $T$  gradient is allowed to stabilize in between these two extremes, along the DNA migration path. When the gel slab is equilibrated in this  $T$  interval, the DNA sample is applied at the cathode and allowed to migrate towards the anode, i.e., towards a progressively higher denaturant values. Such a set-up would have required substantial efforts in a capillary format. Also jacketing the capillary and forcing circulating heating fluid would have required non-negligible efforts. Finally, we took advantage of a thermal theory [40] and of a computer program [41] we had developed in CZE for predicting the inner capillary temperature as a function of a number of experimentally measured parameters. The critical parameters for the success of such a technique were found to be the following: the stability of the viscous sieving polymer, the capillary length, the choice of buffers with the correct conductivity and the choice of thermal gradients with the right slope. We will briefly review here the thermal theory underlying the present methodology. The temperature increments ( $\Delta T$ ) produced inside the capillary by given voltage gradients ( $E$ , in V/cm) can be calculated according to:

$$\Delta T = \lambda_0 E^2 d^2 / 4\chi \quad (1)$$

where  $\lambda_0$  is the buffer specific electric conductivity at a reference temperature (25°C),  $d$  is the capillary diameter and  $\chi$  the thermal conductivity of the buffer solution. All thermal theories assume the buffer conductivity to be linearly dependent on temperature:

$$\lambda = \lambda_0 [1 + \alpha(T - T_0)] \quad (2)$$

where  $\alpha$  is the temperature coefficient of conductivity and  $T$  is the temperature inside the capillary [40]. Thus, the experimental parameters needed for predicting the temperature increments linked to voltage ramps, are: the capillary diameter, its total length, the Biot number, the electric current values ( $\mu\text{A}$ ) linked to a given applied voltage, the buffer electric conductivity ( $\lambda_0$ , in  $\text{mS/cm}$ ) and its thermal coefficient of conductivity ( $\alpha$ , in  $1/\text{K}$ ) (see Fig. 3, panel a). Given these input parameters, a dedicated software allows precise determination of the capillary inner temperature [41]. Graphs can then be easily constructed linking first voltage ramps with electric current (in  $\mu\text{A}$ ) and then voltage ramps with temperature gradients (see Fig. 3, panel b). The typical experimental parameters finally adopted in most runs were: 100  $\mu\text{m}$  I.D., 375  $\mu\text{m}$  O.D., 50-cm long capillaries, coated with a hydrolytically stable poly(*N*-acryloyl amino ethoxy ethanol, AAEE) [42] (as shown in Fig. 3, but now substituted with poly(AAP)) and filled with a 8.9 mM Tris, 8.9 mM borate, 1 mM EDTA, 10 mM NaCl, 6 M urea buffer (TBE), pH 8.3, containing 6% poly(AAP), polymerized in situ at 25°C, as sieving liquid polymer. The experimentally measured physico-chemical parameters of this buffer are:  $\alpha = 0.019 \pm 0.00035 \text{ K}^{-1}$  and  $\lambda_0 = 0.985 \pm 0.0035 \text{ S/cm}$ . The temperature gradient which is then generated during the run takes into consideration the melting profile of the amplified fragments, as predicted by the dedicated software developed by Lerman and Silverstein [39] and as shown in the example of Fig. 2.

There are a number of rules we have learned when developing the present technique: (a) the sample should be injected in the capillary so as to be maintained (by combined chemical and thermal means) just below the expected  $T_m$  value; (b) the temperature ramp activated should be in general rather narrow (of the order of 1 to 1.5°C); (c) the

sweep slope should be very gentle (typically 0.05°C/min). As a starting condition, the constant denaturant concentration (6 M urea), the low ionic strength of the buffer (8.9 mM TBE) and the correct outside temperature platform at which the capillary is equilibrated, produce a combined (chemical and thermal) denaturant plateau which brings the analyte DNA fragments very close (and just below) their respective  $T_m$  values. As soon as the voltage ramp is generated, the programmed temperature increments, producing sudden mobility decrements of the duplexes which start unwinding along the migration path, allow optimal resolution of the DNA analyte into the characteristic four-band pattern of homo- and heteroduplexes. As it will be shown below, and contrary to what is routinely performed in gel-slab operations (where  $\Delta T$  values along the migration path as high as 15°C are typical), optimum separation in all cases is achieved within a very narrow temperature range (1–1.5°C). The most frequently employed gradients of denaturants used in DGGE have been reproduced in the TGCE mode: 10–60% (low-melters); 20–70% (intermediate-low-melters); 30–80% (intermediate-high-melters) and 40–90% (high-melters).

## 5. Examples of separations of low- to high-melters by non-isocratic CZE

Fig. 4 shows the electropherograms of a PCR-amplified sample of a cystic fibrosis (CF) patient exhibiting two polymorphisms (V868V, T854T/other) in exon 14a (V868V; T854T) of the cystic fibrosis transmembrane conductance regulator (CFTR) gene. The constant-temperature run (lower profile) gives a single peak, representing indeed an envelope of four duplexes, fully-resolved in the temperature-gradient run shown in the upper tracing. Note that in this case the mutant homoduplex (M/M) has the highest melting point, thus it is the first eluting peak, since it is the last one to unwind along the electrophoretic track. This is a typical example of resolution of a low melter, since the upper run occurs in a temperature interval from 45 to 49°C. It should be noted, however, that the real  $T_m$  is considerably higher, since the presence of 6 M urea weakens the hydrogen bonds of the double helix and thus lowers the apparent  $T_m$  by as much as 12°C (2°C/unit of

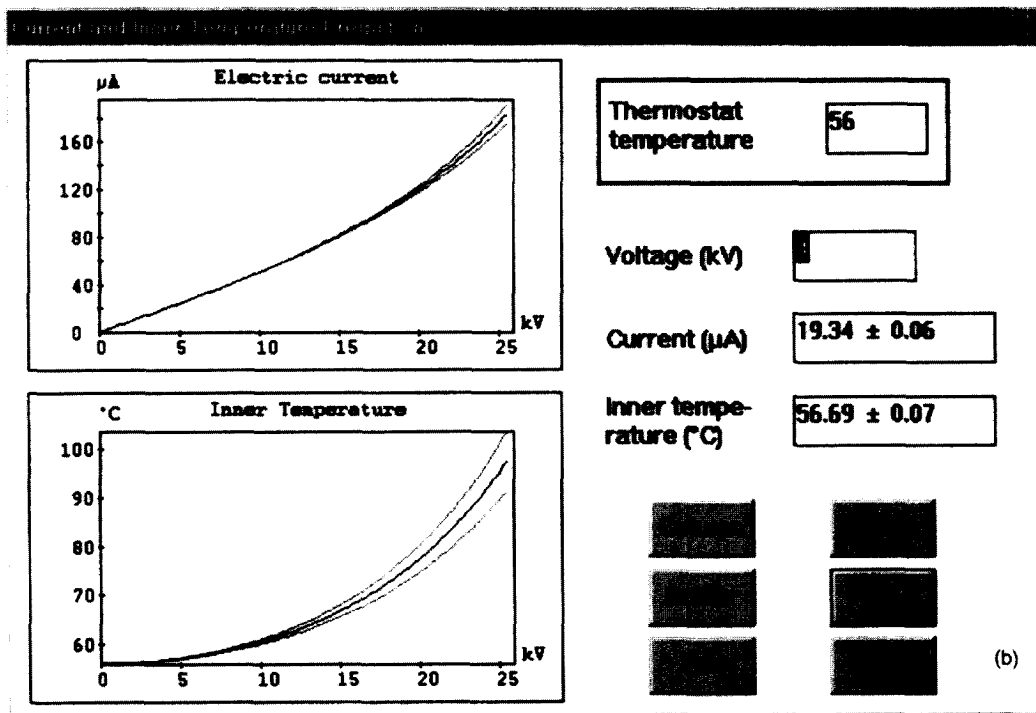
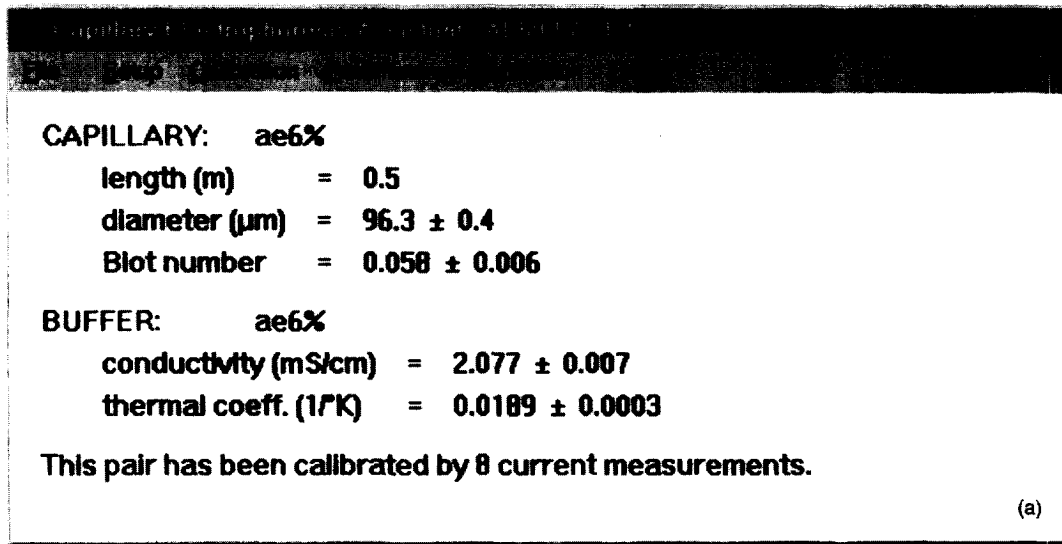


Fig. 3. Method for generating temperature gradients in a capillary. Panel a gives the input parameters for a specific run, divided into capillary parameters (length, diameter and Biot number) and buffer parameters (conductivity and thermal coefficient). Panel b shows graphs for predicting current and temperature inside the capillary lumen corresponding to given voltage ramps. The upper graph links a given voltage profile to the corresponding current generated in the capillary having the parameters shown in panel a. The lower graph links a voltage ramp to a precise temperature generated into the capillary lumen. The thin lines above and below the central, thicker line, represent the standard deviation. The windows to the right exemplify a single point prediction along the curve to the right: given an outside thermostat temperature of  $56^\circ\text{C}$ , at a voltage or 4 kV and at a current of  $19.34 \mu\text{A}$ , the temperature inside the capillary lumen will be  $56.69^\circ\text{C}$  (Gelfi and Righetti, unpublished).

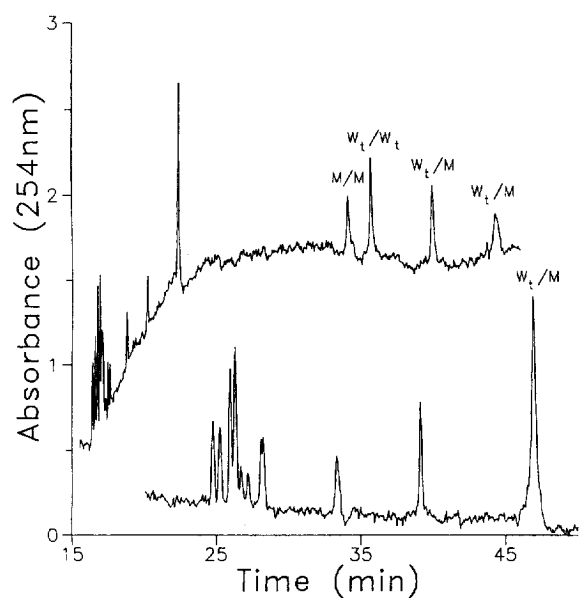


Fig. 4. Electropherograms of a PCR-amplified sample of a CF patient exhibiting two polymorphisms in exon 14a (V868V, T854T/other) on the same chromosome. CZE was run in a Waters Quanta 4000E unit equipped with a 60 cm  $\times$  100  $\mu$ m I.D. capillary, coated with a covalent layer of 6% poly(*N*-acryloylaminoethoxy ethanol; AAEE) and filled with an 8.9 mM TBE buffer, pH 8.3, 1 mM EDTA, 10 mM NaCl in 6 M urea and 8% poly(AAEE) as a liquid sieving polymer matrix. Lower tracing: constant temperature run at 45°C, 6 kV; upper electropherogram: temperature gradient run, from 45 to 49°C, with increments of 0.2°C/min, obtained with a voltage ramp (6 kV start, 22 kV end settings). Note that in the upper tracing the expected four peak pattern is obtained, whereas the single peak in the lower tracing is indeed an envelope of four bands. The early eluting peaks represent unpurified primers and GC-clamp fragments. Detection by UV absorbance at 254 nm (Gelfi et al., see Ref. [43], with permission).

urea molarity). This is one of the earliest runs we made, and it was performed in a quite naive way. As we later learned, it is not wise to perform a separation in such a wide temperature interval, since quite often point mutants have rather minute  $\Delta pI$  values, thus they can only be separated in quite shallow  $T$  gradients.

Fig. 5 shows how important it is to optimize a TCGE run for developing the right four-peak pattern. Here we were running an intermediate to high melter in the CFTR gene (an S1251N mutation in exon 20) [44]. Panel A shows a control run in the absence of a

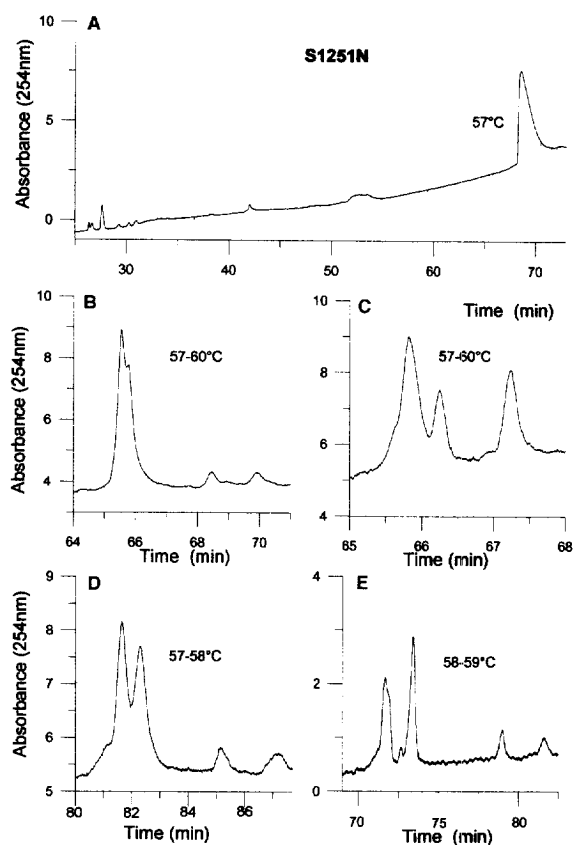


Fig. 5. Results of CZE runs under sub-optimal conditions, as applied to the analysis of the S1251N mutation in exon 20 of the CFTR gene. Sample injection: electrokinetic, 3 s at 4 kV. The standard run (58 to 59°C temperature gradient, 3 to 4 kV voltage ramp, 0.05°C/min sweep rate) is shown in panel E. A: Injection at a constant plateau of 57°C and run in the absence of a temperature gradient. B and C: 57 to 60°C gradient, with a sweep rate of 0.25°C/min (B) or 0.125°C/min (C), over a 3 to 7 kV voltage ramp; D: same as E, but in the 57–58°C interval (Gelfi et al., see Ref. [44], with permission).

temperature gradient, but at a  $T$  value (57°C) very close to the  $T_m$ : only one broad peak is obtained, surely indicative of sample heterogeneity, but of no diagnostic value. If too broad a  $T$  interval is adopted (panel B, 57 to 60°C), with a too steep sweep rate (0.25°C/min) although embracing the  $T_m$  value, the two homo-duplexes are poorly resolved, whereas the two hetero-duplexes are clearly visible in the 68 to 70 min time window. When utilizing the same temperature interval (57–60°C) but with a more



gentle slope (0.125°C/min) (panel C), the two homo-duplexes are well resolved, whereas now the two hetero-duplexes fuse into a single peak eluting at 67 min. If the temperature interval is in the wrong range (panel D, 57 to 58°C interval, centred on the low side of the  $T_m$ ) partial resolution of the two homo- and good resolution of the two hetero-duplexes is achieved. When the  $T$  gradient has the inflection point just right on the  $T_m$  value (panel E), optimum resolution of the four zones is engendered.

Fig. 6 shows the analysis of a set of intermediate-low-melting fragments, amplified from CF patients heterozygous for different mutations in exon 11 of the CFTR gene: 1717-1G→A (panel A); G542X

(G→T at 1756; panel C) and 1784delG (panel D) with their respective normal control (panel E). All mutants exhibit the characteristic four-peak profile, vs. a single band in the control. As shown in the temperature profile of panel B, these mutants are intermediate-low-melters, with  $T_m$  values in the 56.5 to 57.8°C range [44].

Fig. 7 shows the analysis of a high melter, fragment IIIC (319 bp) carrying a G→A transition in IVS-IIInt.1 position of the  $\beta$ -globin gene. Panel A is a control run, at room temperature, in presence of 1.5% HEC as sieving liquid polymer, run at 100 V/cm. Panel B shows the same run, in 1.5% HEC, in the 60–61°C temperature interval, where the envelope of two homo- and two hetero-duplexes is fully resolved. The same occurs in 4% poly(AA) (panel C), in the same temperature interval, with comparable transit times for the four zones. Panel D shows a standard DGGE run in presence of a gradient of chemical denaturant (42–72% formamide); here too the spectrum of four bands is well resolved [45].

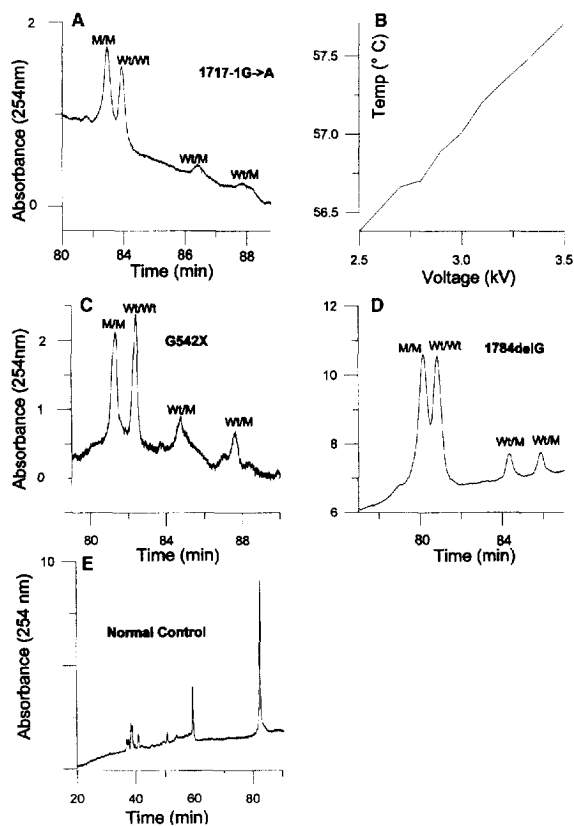


Fig. 6. CZE analysis of 3 mutants in exon 11 of the CFTR gene: 1717-1G→A (panel A); G542X (C) and 1784delG (D); the normal control (NC) is in panel E. All other conditions as in Fig. 5, except that the starting temperature plateau was 56.5°C. B: plot of the temperature profile over the applied voltage ramp (Gelfi et al., see Ref. [44], with permission).

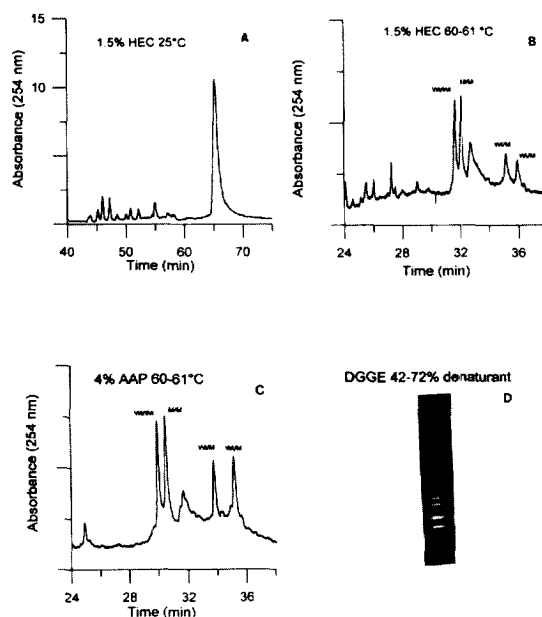


Fig. 7. CZE of fragment IIIC (319 bp), IVS-IIInt.1 of the  $\beta$ -globin gene, carrying a G→A transition. A: Control run, at 25°C, in 1.5% HEC; B: same as A, but in a temperature interval of 60–61°C; C: same as B, but in 4% poly(AAP); D: control run in DGGE (Gelfi et al., see Ref. [45], with permission).

## 6. A glimpse at the future

We have shown above that our non-isocratic CZE is fully capable of resolving a variety of point mutants, even the most tenacious high melters, which require quite drastic conditions for operation. Can we do better than that? A minor flaw of the present technique, quite evident especially in the gel-slab format, is the fact that often the two hetero-duplexes appear as rather broad and often minute peaks. The reason for that is the fact that their  $T_m$  values are not quite so sharp and thus the unwinding occurs over a broader range of denaturing conditions, leading to smearing of the zones. Although in CZE we can still distinguish these peaks, in gel-slab operations the smearing is so severe that, when staining the bands with etidium bromide, their fluorescence cannot quite be distinguished from the faint fluorescence of the background. We have recently reported a novel technique for screening of point mutations in genomic DNA: double gradient (DG) denaturing gradient gel electrophoresis (DGGE) [46]. Unlike conventional DGGE, which exploits a single gradient of denaturing chemicals (typically urea and formamide) along the migration path, in order to force the two hetero- and two homo-duplexes to partially unwind and separate, DG-DGGE overimposes a second gradient to the denaturing one: a porosity gradient. With the help of the sieving gradient, molecules such as the hetero-duplexes, which often produce curtains and smears, instead of sharp zones, due to lack of a sharp melting transition, are re-compacted into remarkably narrow bands. Even homo-duplexes with minute  $T_m$  differences, giving a single band in DGGE, are resolved into two zones in DG-DGGE. The technique has been applied to the analysis of a number of point mutations in several exons of the CFTR gene [46]. The question is how to implement such double gradients (or for that matter even triple: of porosity, of chemical and of thermal denaturants!) in a capillary format. We hope to be able to give an answer to such a non-trivial question in the afternoon edition of this journal!

## 7. List of abbreviations and symbols

$\alpha$  Temperature coefficient of conductivity

AAEE	<i>N</i> -Acryloyl aminoethoxy ethanol
AAP	<i>N</i> -Acryloyl aminopropanol
$\chi$	Thermal conductivity
CF	Cystic fibrosis
CFTR	Cystic fibrosis transmembrane regulator (gene)
CZE	Capillary zone electrophoresis
<i>d</i>	Capillary diameter
DGGE	Denaturing gradient gel electrophoresis
ds	Double stranded (DNA)
EDTA	Ethylene diamine tetra acetate
HEC	Hydroxyethyl cellulose
HPMC	Hydroxypropylmethyl cellulose
$\lambda_0$	Buffer specific electric conductivity
M	Mutant
MC	Methyl cellulose
$M_n$	Number—average molecular mass (for polymers)
$M_w$	Weight—average molecular mass (for polymers)
PCR	Polymerase chain reaction
PEG	Poly(ethylene glycol)
PEO	Poly(ethylene oxide)
ss	Single stranded (DNA)
<i>T</i>	Temperature
TBE	Tris borate EDTA (buffer)
TGCE	Thermal gradient capillary electrophoresis
TGGE	Thermal gradient gel electrophoresis
$T_m$	Melting point
VNTR	Variable number of tandem repeats
$W_t$	Wild-type

## Acknowledgments

P.G.R. is supported by a grant from AIRC (Associazione Italiana Ricerca sul Cancro), the European Community (Bio Med 2, Grant No. BMH4-CT96-1158), by Consiglio Nazionale delle Ricerche (CNR, Roma, Progetto Strategico Tecnologie Chimiche Innovative No. 95.04567.ST74 and by Comitato Tecnologico) and by Telethon Italy (Grant No. E-153).

## References

- [1] J.C. Kaplan and M. Delpech, *Biol. Mol. Med.*, Flammarion, Paris, 1993.

- [2] P.G. Righetti (Editor), *Capillary Electrophoresis in Analytical Biotechnology*, CRC Press, Boca Raton, FL, 1996.
- [3] X.C. Huang, M.A. Quesada and R.A. Mathies, *Anal. Chem.*, 64 (1992) 967–972.
- [4] S.M. Clark and R.A. Mathies, *Anal. Biochem.*, 215 (1993) 163–170.
- [5] K. Ueno and E.S. Yeung, *Anal. Chem.*, 66 (1994) 1424–1431.
- [6] A.T. Woolley and R.A. Mathies, *Proc. Natl. Acad. Sci. USA*, 91 (1994) 11 348–11 352.
- [7] A.T. Wooley and R.A. Mathies, *Anal. Chem.*, 67 (1995) 3676–3680.
- [8] C. Gelfi, M. Perego and P.G. Righetti, *Electrophoresis*, 17 (1996) 1470–1475.
- [9] N.J. Dovichi (Editor), *Paper Symposium: Nucleic Acid Electrophoresis*, *Electrophoresis*, 17, 1996, pp. 1407–1517.
- [10] P.G. Righetti and C. Gelfi, in P.G. Righetti (Editor), *Capillary Electrophoresis in Analytical Biotechnology*, CRC Press, Boca Raton, FL, 1996, pp. 431–476.
- [11] Y. Baba, *J. Chromatogr. B*, 687 (1996) 271–302.
- [12] M. Strega and A. Lagu, *Anal. Chem.*, 63 (1991) 1233–1236.
- [13] Y. Baba, N. Ishimaru, K. Samata and M. Tshako, *J. Chromatogr. A*, 653 (1993) 329–335.
- [14] D.A. McGregor and E.S. Yeung, *J. Chromatogr. A*, 652 (1993) 67–73.
- [15] P.D. Grossman and D.S. Soane, *J. Chromatogr.*, 559 (1991) 257–266.
- [16] M.H. Kleemiss, M. Gilges and G. Schomburg, *Electrophoresis*, 14 (1993) 515–522.
- [17] A.E. Barron, H.W. Blanch and D.S. Soane, *Electrophoresis*, 15 (1994) 597–615.
- [18] A.E. Barron, W.M. Sunada and H.W. Blanch, *Electrophoresis*, 16 (1995) 64–74.
- [19] H.E. Schawartz, K. Ulfelder, F.J. Sanzeri, M.P. Busch and R.G. Brownlee, *J. Chromatogr.*, 559 (1991) 267–283.
- [20] H.T. Chang and E.S. Yeung, *J. Chromatogr. B*, 669 (1995) 113–123.
- [21] P. Bocek and A. Chrambach, *Electrophoresis*, 12 (1991) 1059–1061.
- [22] S. Hjertèn, T. Srichaivo and A. Palm, *Biomed. Chromatogr.*, 8 (1994) 73–78.
- [23] T. Izumi, M. Yamaguchi, K. Yoneda, T. Isobe, T. Okuyama and T. Shinoda, *J. Chromatogr.*, 652 (1993) 41–50.
- [24] D.N. Heiger, A.S. Cohen and B.L. Karger, *J. Chromatogr.*, 516 (1990) 33–44.
- [25] C. Gelfi, A. Orsi, F. Leoncini and P.G. Righetti, *J. Chromatogr. A*, 689 (1995) 97–107.
- [26] M. Chiari, M. Nesi and P.G. Righetti, *Electrophoresis*, 15 (1994) 616–622.
- [27] E. Simò-Alfonso, C. Gelfi, R. Sebastiano, A. Citterio and P.G. Righetti, *Electrophoresis*, 17 (1996) 723–731.
- [28] E. Simò-Alfonso, C. Gelfi, R. Sebastiano, A. Citterio and P.G. Righetti, *Electrophoresis*, 17 (1996) 732–737.
- [29] C. Gelfi, E. Simò-Alfonso, R. Sebastiano, A. Citterio and P.G. Righetti, *Electrophoresis*, 17 (1996) 738–743.
- [30] E. Simò-Alfonso, C. Gelfi, M. Lucisano and P.G. Righetti, *J. Chromatogr. A*, 756 (1996) 255–261.
- [31] C. Gelfi, M. Perego, F. Libbra and P.G. Righetti, *Electrophoresis*, 17 (1996) 1342–1347.
- [32] J.Z. Zhang, Y. Fang, J.Y. Hou, J.H. Ren, R. Jiang, P. Roos and N.J. Dovichi, *Anal. Chem.*, 67 (1995) 4589–4593.
- [33] S. Menchen, B. Johnson, M.A. Winnik and B. Xu, *Electrophoresis*, 17 (1996) 1451–1459.
- [34] A.P. Sassi, A. Barron, M.G. Alonso-Amigo, D.Y. Hion, J.S. Yu, D.S. Soane and H.H. Hooper, *Electrophoresis*, 17 (1996) 1460–1469.
- [35] A.R. Isenberg, B.R. McCord, B.W. Koons, B. Budowle and R.O. Allen, *Electrophoresis*, 17 (1996) 1505–1511.
- [36] R.M. Myers, T. Maniatis and L. Lerman, *Methods Enzymol.*, 155 (1987) 501–527.
- [37] D. Riesner, K. Henco and G. Steger, *Adv. Electrophoresis*, 4 (1991) 169–250.
- [38] M. Grompe, *Nature Genet.*, 5 (1993) 111–117.
- [39] L. Lerman and K. Silverstein, *Methods Enzymol.*, 155 (1987) 482–501.
- [40] M.S. Bello, M. Chiari, M. Nesi and P.G. Righetti, *J. Chromatogr. B*, 652 (1992) 323–330.
- [41] M.S. Bello, E.I. Levin and P.G. Righetti, *J. Chromatogr. A*, 652 (1993) 329–336.
- [42] M. Chiari, C. Micheletti, M. Nesi, M. Fazio and P.G. Righetti, *Electrophoresis*, 15 (1994) 177–186.
- [43] C. Gelfi, P.G. Righetti, L. Cremonesi and M. Ferrari, *Electrophoresis*, 15 (1994) 1506–1511.
- [44] C. Gelfi, P.G. Righetti, L. Cremonesi and M. Ferrari, *BioTechniques*, 21 (1996) 926–932.
- [45] C. Gelfi, P.G. Righetti, M. Travi and S. Fattore, *Electrophoresis*, 18 (1997) in press.
- [46] L. Cremonesi, S. Firpo, M. Ferrari, P.G. Righetti and C. Gelfi, *BioTechniques*, 22 (1997) in press.